

# A Bamboo-Inspired Nanostructure Design for Flexible, Foldable, and Twistable Energy Storage Devices

Yongming Sun,<sup>†,‡</sup> Ryan B. Sills,<sup>§,||</sup> Xianluo Hu,<sup>\*,†</sup> Zhi Wei Seh,<sup>‡</sup> Xu Xiao,<sup>⊥</sup> Henghui Xu,<sup>†</sup> Wei Luo,<sup>†</sup> Huanyu Jin,<sup>⊥</sup> Ying Xin,<sup>#</sup> Tianqi Li,<sup>⊥</sup> Zhaoliang Zhang,<sup>#</sup> Jun Zhou,<sup>⊥</sup> Wei Cai,<sup>§</sup> Yunhui Huang,<sup>\*,†</sup> and Yi Cui<sup>\*,‡,○</sup>

<sup>†</sup>State Key Laboratory of Materials Processing and Die & Mold Technology, School of Materials Science and Engineering and <sup>⊥</sup>Wuhan National Laboratory for Optoelectronics (WNLO), and College of Optoelectronic Science and Engineering, Huazhong University of Science and Technology, Wuhan 430074, P. R. China

<sup>‡</sup>Department of Materials Science and Engineering and <sup>§</sup>Department of Mechanical Engineering, Stanford University, Stanford, California 94305, United States

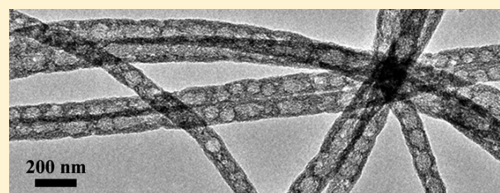
<sup>||</sup>Sandia National Laboratories, Livermore, California 94551, United States

<sup>#</sup>School of Chemistry and Chemical Engineering, University of Jinan, Jinan 250022, P. R. China

<sup>○</sup>Stanford Institute for Materials and Energy Sciences, SLAC National Accelerator Laboratory, 2575 Sand Hill Road, Menlo Park, California 94025, United States

## S Supporting Information

**ABSTRACT:** Flexible energy storage devices are critical components for emerging flexible electronics. Electrode design is key in the development of all-solid-state supercapacitors with superior electrochemical performances and mechanical durability. Herein, we propose a bamboo-like graphitic carbon nanofiber with a well-balanced macro-, meso-, and microporosity, enabling excellent mechanical flexibility, foldability, and electrochemical performances. Our design is inspired by the structure of bamboos, where a periodic distribution of interior holes along the length and graded pore structure at the cross section not only enhance their stability under different mechanical deformation conditions but also provide a high surface area accessible to the electrolyte and low ion-transport resistance. The prepared nanofiber network electrode recovers its initial state easily after 3-folded manipulation. The mechanically robust membrane is explored as a free-standing electrode for a flexible all-solid-state supercapacitor. Without the need for extra support, the volumetric energy and power densities based on the whole device are greatly improved compared to the state-of-the-art devices. Even under continuous dynamic operations of forceful bending (90°) and twisting (180°), the as-designed device still exhibits stable electrochemical performances with 100% capacitance retention. Such a unique supercapacitor holds great promise for high-performance flexible electronics.



**KEYWORDS:** Bamboo-like carbon nanofibers, mechanical properties, supercapacitor, electrochemical performances

Flexible electronics is aimed to be portable, lightweight, bendable, foldable, twistable, and even wearable. Due to these features, the corresponding power sources should be lightweight and stable under different mechanical deformation conditions. Recently, much progress has been made in the development of flexible all-solid-state supercapacitors for flexible electronics owing to their ease of handling, small size, and safety.<sup>1–7</sup> The main limitations, however, are their low volumetric energy density and limited mechanical durability.<sup>8–12</sup> A typical fabrication procedure of an all-solid-state supercapacitor includes the synthesis of active materials on a conductive and flexible substrate, followed by assembly into devices using a gel electrolyte. However, little emphasis has been placed on the development of free-standing flexible active materials without the need for extra support, which is vital for the improvement of energy and power densities based on the volume of the whole devices. In this respect, some progress has

been made in the design of graphene-based film electrodes for all-solid-state supercapacitors.<sup>1,13,14</sup> Carbon nanotube architectures have also been successfully designed as mechanical support to develop fiber type supercapacitors with superior mechanical durability.<sup>3,15,16</sup> In spite of this progress, the energy density of the devices is still limited by the use of flexible but inert substrates or the large proportion of the low-specific-capacitance carbon nanotubes. In other words, an ideal electrode material for flexible all-solid-state supercapacitors should possess high specific capacitance and be highly flexible by itself without the need for mechanical support. However, to date, there are very few successful examples of such all-solid-

**Received:** February 24, 2015

**Revised:** April 15, 2015

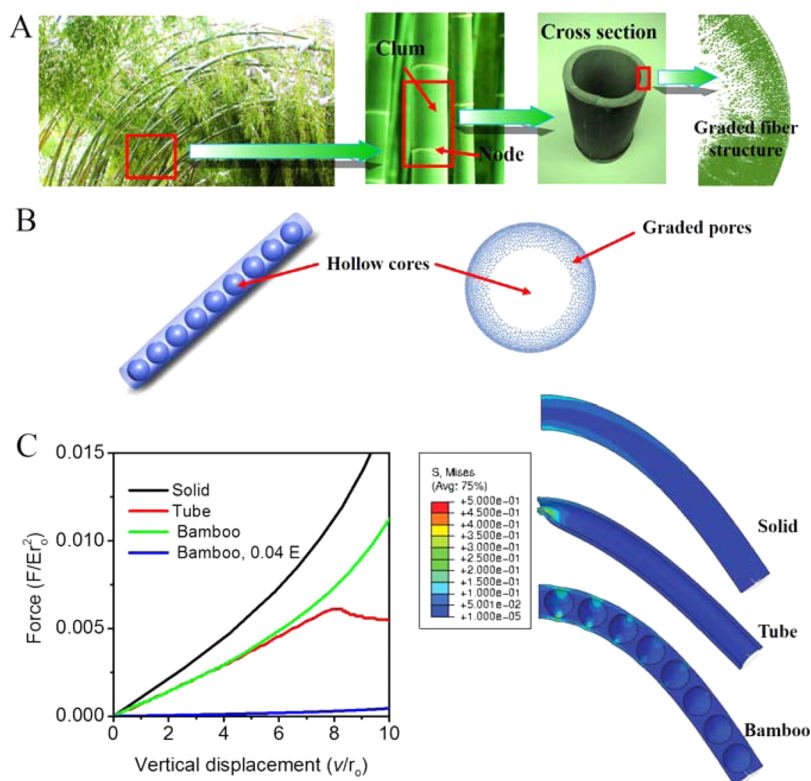


**Figure 1.** Schematic of the bamboo-inspired nanostructure design and three-point bending simulations. (a) The graded structure of bamboos. (b) Schematic of the bamboo-inspired nanostructure design. (c) Results from three-point bending simulations of different fiber geometries: solid fiber, tube, bamboo-like fiber with hollow cores (Bamboo), and fully porous bamboo-like fiber with both hollow cores and graded pores through the cross section (Bamboo, 0.04 E). (Left) The force–displacement response of the nanofibers ( $F$  is the force,  $E$  is Young’s modulus,  $r_0$  is the outer radius). (Right) Snapshots of the deformation and von Mises stress distribution (normalized by the Young’s modulus) at vertical displacements of  $v/r_0 = 10$  ( $v$  is the vertical displacement). The simulation results indicate that bamboo-like nanofibers have much better mechanical durability and flexibility than the solid fibers and tubes.

state supercapacitors showing stable electrochemical performances under continuous dynamic mechanical deformation conditions.

Bamboo is a representative example of plants that possess superior flexibility and mechanical durability. Its geometry consists of a functionally graded structure from macroscopic scale to microscopic scale that is adapted to withstand the forces of nature: The “nodes” provide additional reinforcement for the “culm”, preventing buckling due to bending and axial cracks. The graded structure of the fibers through their cross-section accommodates the stress distribution due to a bending moment and thus optimizes the flexural properties (Figure 1a).<sup>17–19</sup> Here, inspired by the structure of bamboo, we demonstrate a novel, multiscale, hierarchical carbon nanostructure. Such a design has the following characteristics: 1D graphitic carbon nanofibers with uniform discontinuous hollow interiors (macropores) as well as graded nanopores (mesopores and micropores) through the cross-section of the nanofibers (Figure 1b). These hierarchical and well-balanced macro-, meso- and microporosities help to provide a high ion-accessible surface area and low ion transport resistance, which are the keys to achieving high specific capacitance and rate capability in electrical double-layer capacitors.<sup>20–24</sup> Meanwhile, superior mechanical durability and flexibility can also be expected in terms of the unique pore structure. The micro/mesopores account for 79% of the porosity (based on high-resolution nitrogen-sorption analyses discussed later). According to theoretical<sup>25</sup> and empirical<sup>26</sup> estimates, they act to reduce the

global elastic modulus of the nanofibers, the parameter that controls the deformation response to loading over length scales much larger than the micro/mesopore diameters, to approximately 4% of the base material’s value (Supporting Information, Method S1). This reduction in the global modulus results in an overall reduction in stiffness of the nanofibers, making the load required to sustain the same amount of deformation about a factor of 20 lower. Second, the macropores that give the nanofibers their bamboo-like hollow cores also act to reduce the stiffness both globally, by lowering the overall moment of inertia, and locally, by providing thin, flexible regions at the walls of the pores. Additionally, the reinforcement provided by the webs of material separating the macropores give the bamboo-like nanofibers the important property of robustness against localized deformation. To demonstrate this effect, a series of three-point bending simulations were conducted for a solid fiber, a bamboo-like fiber, and a tubular fiber of equivalent moment of inertia to the bamboo-like fiber (Figure 1c, Supporting Information, Method S2). Clearly the stiffnesses of the bamboo-like and tubular fibers are reduced relative to the solid fiber. Additionally, we see that in the case of the tubular fiber, the deformation becomes highly localized as the tube “crimps” together. In contrast, the bamboo-like fiber maintains the same cross-sectional form at the site of loading, indicating it is much more robust. Hence, we believe the bamboo-like fibers are much better at sharing/shedding load in the 2D webs comprising the supercapacitors without inducing localized failure.

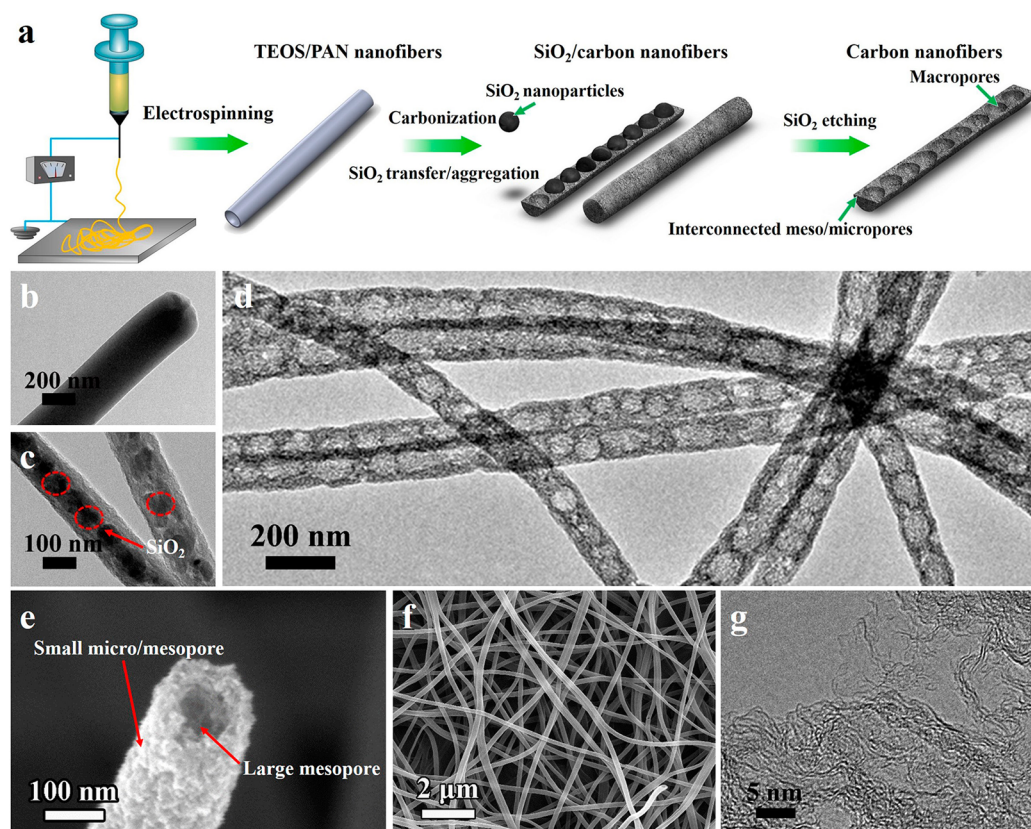


**Figure 2.** Fabrication and characterization of the bamboo-like carbon nanofibers. (a) Schematic of the fabrication process of the bamboo-like carbon nanofibers. TEOS/PAN composite nanofibers were first prepared by electrospinning. By heating the precursors at 1200 °C in a H<sub>2</sub>/Ar (5/95 in volume) atmosphere, ultrafine SiO<sub>2</sub> clusters transfer and aggregate into much larger SiO<sub>2</sub> particles uniformly lined in the core region within the nanofibers, while their transfer path forms interconnected and graded meso/micropores. The bamboo-like nanofibers are finally obtained after removing the SiO<sub>2</sub> particles in a HF aqueous solution. (b,c,d) TEM images of the initial TEOS/PAN composite nanofibers (b), SiO<sub>2</sub>/carbon composite nanofibers (c) and bamboo-like carbon nanofibers (d). The circles in (c) show the existence of SiO<sub>2</sub> particles in the core of the SiO<sub>2</sub>/carbon composite nanofibers. (e,f,g) SEM images (e,f) and HRTEM image (g) of the as-prepared carbon nanofibers.

The schematic of the fabrication process of the bamboo-like carbon nanofibers is shown in Figure 2a. In a typical procedure, a precursor of polyacrylonitrile (PAN) and tetraethyl orthosilicate (TEOS) in dimethylformamide (DMF) was made into a white nanofiber web by electrospinning (Supporting Information, Figures S1 and S2). Black carbon nanofiber network electrodes were then obtained after thermal treatment of these TEOS/PAN nanofiber webs in a H<sub>2</sub>/Ar (5/95 in volume) atmosphere followed by etching SiO<sub>2</sub> in an aqueous HF solution (Supporting Information, Figure S3). The SiO<sub>2</sub> molecular clusters are very uniformly distributed within the as-electrospun nanofibers (Figure 2b). In the heat treatment process, these ultrafine SiO<sub>2</sub> clusters transfer inward and aggregate into much larger SiO<sub>2</sub> particles (tens of nanometers in size) in the center of the nanofibers (Figure 2c, Supporting Information, Figure S4), while their transfer path forms a graded and interconnected pore structure within the shell of the hybrid nanofibers, accompanied by the carbonization of PAN. Etching these SiO<sub>2</sub> particles generates a sequence of spherical holes uniformly distributed along the axes of the nanofibers (Figure 2d). These hollow interiors, together with a graded and interconnected pore structure: small micro/mesopores in the outer surface and larger mesopores in the inner region of the shell (Figure 2e), endow the as-synthesized carbon nanofibers with a unique porous architecture. Meanwhile, these bamboo-like carbon nanofibers

interconnect with each other, forming a tight 2D web with submicron/micron size interfiber porosity (Figure 2f). The pore-size distribution, pore volume, and specific surface area (SSA) of the carbon nanofibers were studied using high-resolution nitrogen-sorption experiments with advanced methods based on density functional theory (DFT) (Supporting Information, Figure S5). The bamboo-like carbon nanofibers have a continuous pore-size distribution from 0.64 nm to over 100 nm. Their SSA is as high as ~1912 m<sup>2</sup> g<sup>-1</sup>, and their pore volume is ~2.27 cm<sup>3</sup> g<sup>-1</sup>. Furthermore, their porosity and SSA can be tuned easily by controlling the diffusion of the SiO<sub>2</sub> clusters in the fibers (Supporting Information, Figures S6 and S7), indicating great versatility in manipulating the pore structure. A high resolution transmission electron microscopy (HRTEM) image shows that the shells of these bamboo-like carbon nanofibers consist of interconnected and highly curved graphitic carbon nanosheets, supporting their superior structural flexibility and electrical conductivity (Figure 2g). Detailed structure characterization, including electron energy loss spectroscopy (EELS), powder X-ray diffraction (XRD), X-ray photoelectron spectroscopy (XPS), elemental analysis, and Raman spectroscopy (Supporting Information, Figures S8–S11), further confirm their graphitic carbon structure.

Due to the bamboo-like fiber structure and tight organization of the 2D fibrous felts, our carbon nanofiber network electrode is flexible, foldable, and pliable. The prepared carbon

membrane recovers its initial state easily after 3-folded manipulation, indicating its excellent mechanical durability (Figure 3a, Supporting Information, Movie S1). Figure 3b

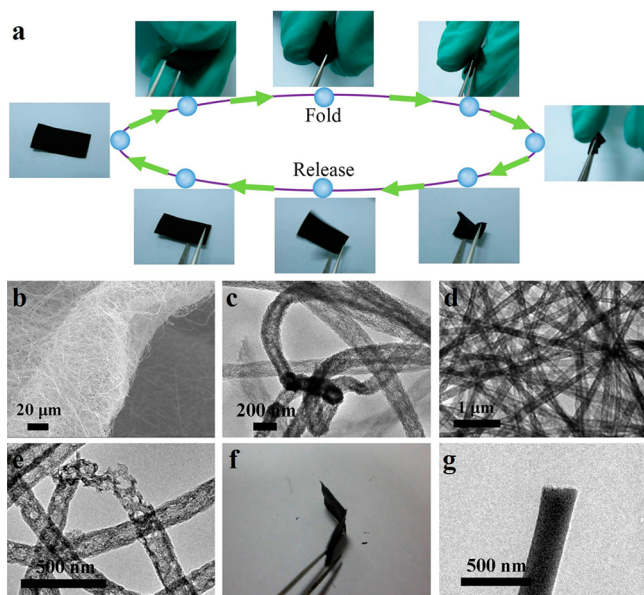


**Figure 3.** Mechanical properties and structural characterizations of the as-obtained bamboo-like carbon nanofiber webs. (a) A piece of carbon nanofiber web is 3-folded and recovers its initial state easily, indicating its excellent mechanical durability. More detailed information on the mechanical durability of the as-prepared bamboo-like carbon nanofiber webs under dynamic forceful operations can be seen in Supplementary Movie 1. (b) SEM images of a piece of carbon nanofiber web with a bending angle of  $180^\circ$ . (c,d) TEM images of carbon nanofibers from a membrane that is folded ( $180^\circ$ ), twisted ( $180^\circ$ ), extruded, and sandwiched between two TEM grids (c) and their recover after the release of strain (d). (e) TEM image of a damaged bamboo-like carbon nanofiber, which retains connected remnants. (f) Digital picture of a membrane of solid fibers failed under a small bending angle ( $<50^\circ$ ). (g) TEM image of a failed solid fiber, which shows a flat fractured cross section.

shows a SEM image of a carbon nanofiber web with a bending angle of  $180^\circ$ , demonstrating that the structure of bamboo-like nanofibers remain without any damage. Furthermore, TEM measurement was carried out to observe the mechanical durability of the bamboo-like carbon nanofibers. Before observation, a carbon fiber web was folded ( $180^\circ$ ), twisted ( $180^\circ$ ), extruded, and sandwiched between two TEM copper grids. It was confirmed that the fibrous structure was well maintained even after being highly bent and twisted (Figure 3c). After being unloaded, the fibers recover their initial states, indicating extraordinary mechanical flexibility, foldability and twistability (Figure 3d). To study the fracture mechanism of our bamboo-like carbon nanofibers, we bent, twisted and stretched a piece of carbon nanofiber web forcefully and observed it under a TEM (Figure 3e). Interestingly, our carbon nanofibers did not break by cleavage fracture. Damaged fibers were observed to retain connected remnants, indicating a dissipative fracture process. For comparison, we prepared a membrane comprising of carbon nanofibers with negligible porosity and SSA, and a bending operation was also carried out. With a very small bending angle ( $<50^\circ$ ), the web of solid carbon nanofibers fractured easily (Figure 3f, Supporting

Information, Movie S2), and a flat cross-section was observed (Figure 3g), indicating a brittle fracture process.

Here, the capacitive properties of the bamboo-like carbon nanofiber webs were explored by using a traditional three-electrode configuration in a liquid electrolyte (Figure 4). Figure 4a and b shows the typical cyclic voltammetry (CV) curves at various scan rates between 10 and  $2000 \text{ mV s}^{-1}$ , within the potential range of  $-0.9$  to  $0 \text{ V}$  (vs Hg/HgO). Rectangular shapes of the CVs are obtained even at a very high scan rate of  $2000 \text{ mV s}^{-1}$ , indicating a very fast and efficient charge transfer. Figure 4c shows the nearly triangular shape of the galvanostatic charge/discharge curves obtained at a high current density of  $100 \text{ A g}^{-1}$ , suggesting the formation of efficient electrochemical double layers and fast ion transport within the carbon nanofiber electrodes. The as-made carbon nanofiber electrodes exhibit an outstanding specific capacitance as high as  $236 \text{ F g}^{-1}$  at a current density of  $5 \text{ A g}^{-1}$  and show a very small decrease in gravimetric capacitance even at very high current densities ( $\sim 30\%$  at  $100 \text{ A g}^{-1}$ ) (Figure 4c and d). Meanwhile, the electrodes also display an extraordinarily high stability with  $\sim 100\%$  of the initial capacitance after 5000 cycles tested at a constant current density of  $10 \text{ A g}^{-1}$  (Figure 4e). Our bamboo-like carbon nanofiber web, possessing inherent 3D interconnected hierarchical porous structures with high SSA, evidently supports its potential applications for high-performance supercapacitors. The large and accessible SSA to the electrolyte enables high specific capacitance. The superior rate capability can be ascribed to the highly conductive pathway for electrons and fast transport channels for ions. Previous studies indicated that the power characteristics of many carbon materials remains limited due to an intrinsically high fraction of microporosity, which in turn limits pore accessibility of the electrolyte ions at high current densities.<sup>27</sup> Here, our bamboo-like porous carbon nanoarchitecture is successful in achieving high power density as well as keeping high energy density by creating facile electron/ion-transport pathways. With the combination of superior electrochemical properties and mechanical durability, the bamboo-like carbon nanofiber webs are promising candidates for flexible all-solid-state supercapacitor electrodes.

To explore the electrochemical performances of the as-synthesized bamboo-like carbon nanofiber webs as all-solid-state supercapacitor electrodes, symmetric supercapacitors can be readily made by sandwiching a cellulose separator between two identical carbon nanofiber web electrodes. The free-standing carbon nanofiber webs serve as both the active material and current collector in the two-electrode cell configuration because of their good conductivity. Moreover, the as-made devices do not require any flexible substrates (e.g., polyethylene terephthalate substrate, conductive aluminum foil, and nitrocellulose membrane) due to the superior mechanical durability of the bamboo-like carbon nanofiber webs. The thickness of devices is tunable by selecting carbon nanofiber webs with different thicknesses, making them potentially useful in microdevice applications.<sup>28</sup> It has been recognized that supercapacitor electrodes comprising of an active material coating layer on flexible conductive support (e.g., a carbon cloth) and an active thin film on a flexible substrate (e.g., polyethylene terephthalate) usually have a smaller internal resistance and better ion diffusion characteristics to achieve a higher apparent specific capacitance when normalized by the weight of the active materials. However, high energy and power densities cannot always be obtained on the basis of the total volume or weight of the devices due to the presence of inactive

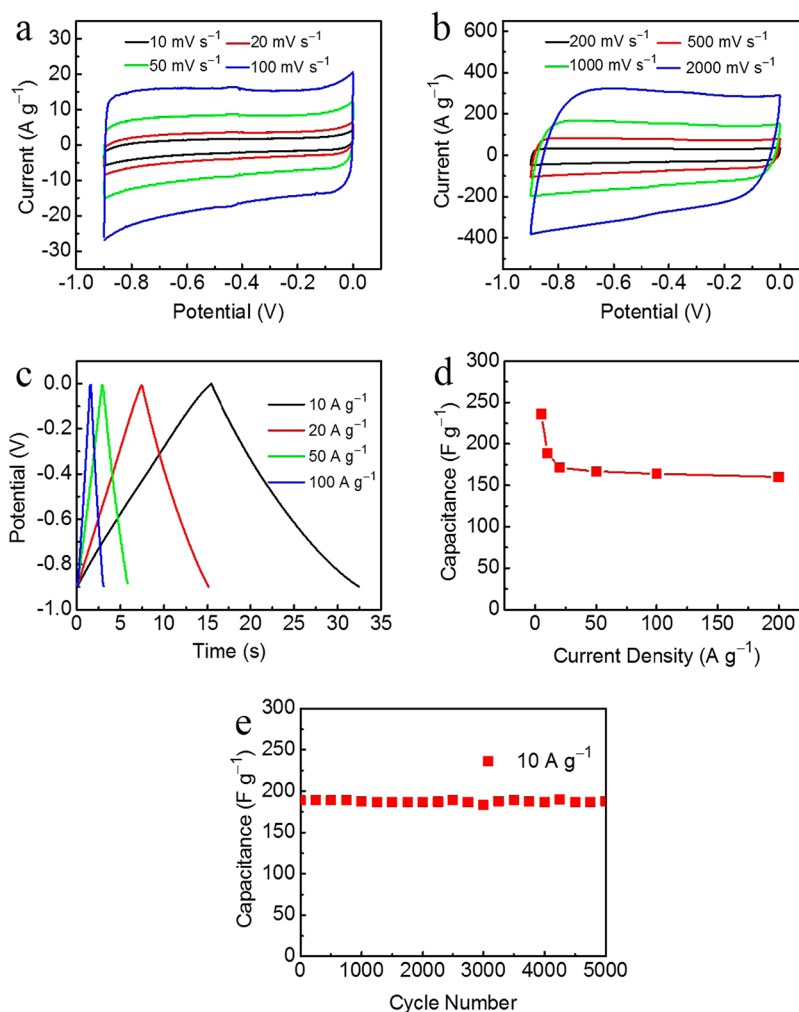


**Figure 4.** Electrochemical performances of a free-standing carbon nanofiber electrode using a conventional three-electrode configuration. (a,b) CV curves of a carbon nanofiber electrode between 10 and 2000 mV s<sup>-1</sup>. (c) The galvanostatic charge/discharge curves at current densities of 10, 20, 50, and 100 A g<sup>-1</sup>. (d) The specific capacitances calculated from the discharge curves at different current densities. (e) Cyclic stability of a carbon electrode at a current density of 10 A g<sup>-1</sup>.

current collectors or flexible substrates. In this respect, the content ratio of the active materials in the as-made devices is greatly increased, which leads to the increase of energy and power densities based on the entire devices. The electrochemical performances of the as-made devices were tested after the gel electrolyte dried and all of the measurements were based on the total volume of the devices. The capacitive performance of the flexible all-solid-state supercapacitors was first evaluated by CV measurements. Figure 5a and b shows the CV curves of the device at various scan rates with voltage windows ranging from 0 to 0.9 V. In general, the shape of the CV loop of an ideal electrical double-layer supercapacitor should be rectangular. The CV curves of our device are close to rectangular even at a high scan rate of 2000 mV s<sup>-1</sup>, demonstrating an excellent capacitive behavior and a fast charge/discharge property. Typical galvanostatic charge/discharge curves are shown in Figure 5c. The linear profile of galvanostatic charge/discharge curves and their symmetric triangular shape indicate nearly ideal capacitive characteristics. The device exhibits a high specific capacitance of 2.1 F cm<sup>-3</sup> at 33 mA cm<sup>-3</sup>. This result is much higher than those of well-designed carbonaceous supercapacitors reported in the literature (e.g., 0.45 F cm<sup>-3</sup> based on graphene film electrodes<sup>1</sup>

and 1.3 F cm<sup>-3</sup> with onion-like carbon electrodes<sup>29</sup>) and, even higher than or comparable to those of some metal oxide-based supercapacitors (e.g., 0.7 F cm<sup>-3</sup> based on H-TiO<sub>2</sub>@MnO<sub>2</sub> and H-TiO<sub>2</sub>@C electrodes,<sup>30</sup> and 2.5 F cm<sup>-3</sup> based on carbon/MnO<sub>2</sub> core-shell fiber electrodes<sup>31</sup>). Moreover, the capacitance remains 1.6 F cm<sup>-3</sup> at 3333 mA cm<sup>-3</sup>, demonstrating a good rate capability (Figure 5d). The high-rate performance of this device can be attributed to the following aspects: (i) The hierarchical porous structure of the carbon nanofiber webs effectively adsorbs the gel electrolyte and minimizes the ion diffusion distance and transport resistance;<sup>32</sup> (ii) The interconnected conductive network builds up an express path for ultrafast electron transport; (iii) Additional polymer binders are not used, which commonly introduce extra contact resistance and dead weight. The fast ion transport within the carbon nanofiber electrodes was confirmed by the result of electrochemical impedance spectroscopy (EIS) (Supporting Information, Figure S12). Additionally, the flexible all-solid-state supercapacitors show a stable cycle life in the potential range of 0–0.9 V at 67 mA cm<sup>-3</sup> and retain 96% of the initial capacitance after 10 000 cycles, indicating excellent cycling stability (Figure 5e). Power and energy densities are two important parameters for evaluating the electrochemical

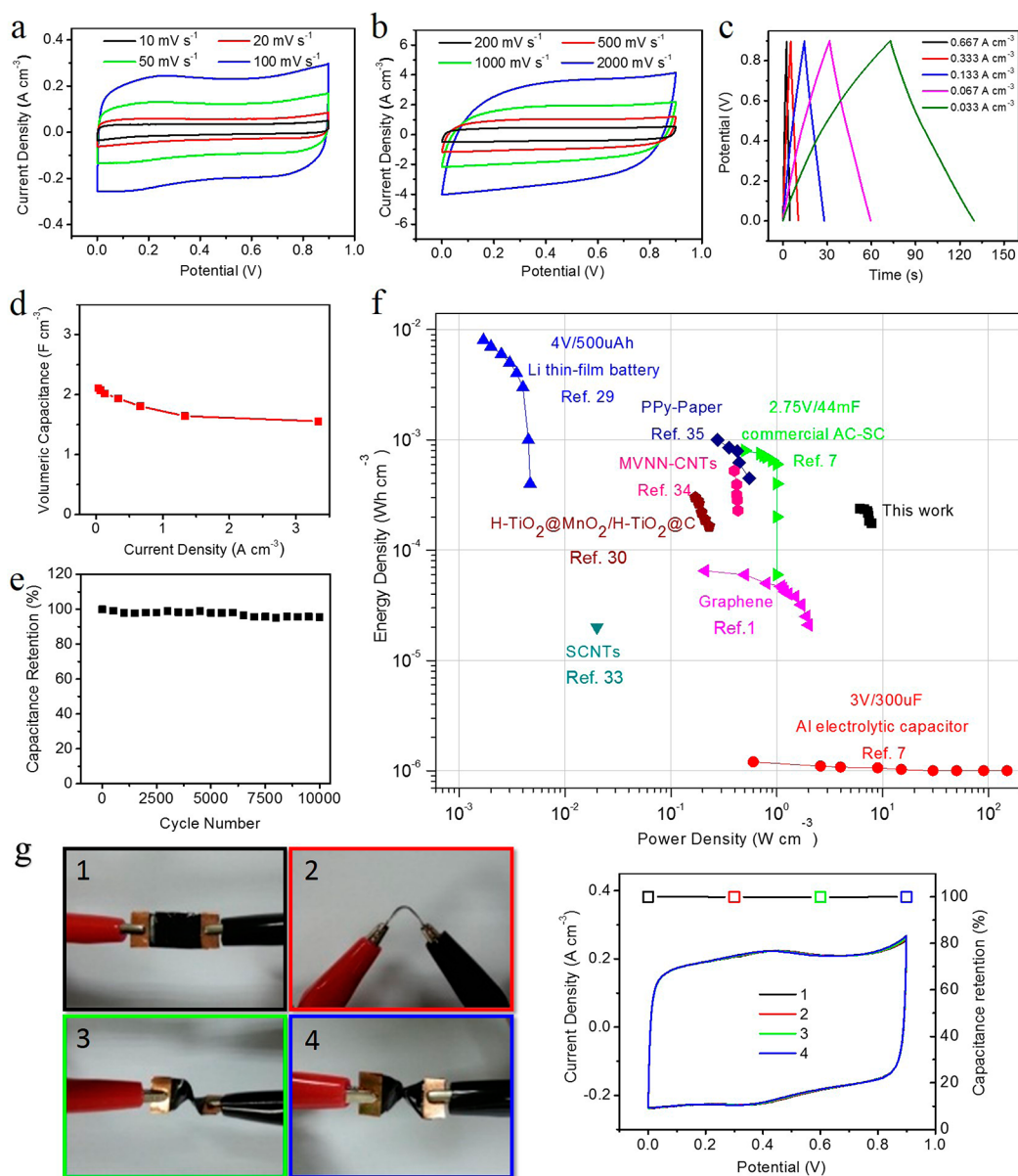


**Figure 5.** Electrochemical performances of a typical all-solid-state flexible supercapacitor. (a,b) CV curves. (c) Galvanostatic charge/discharge curves. (d) Volumetric capacitance with respect to scan rates. (e) Cycle life. (f) Ragone plot. (g) Electrochemical behaviors of the as-made all-solid-state supercapacitor under different mechanical deformation conditions. (Left) Digital images of the flexible device bended by (1) 0° and (2) 90°, and twisted by (3) 90° and (4) 180° and (right) the corresponding CV curves and capacitance retention tested at 100 mV s<sup>-1</sup>. Our all-solid-state device exhibits superior stable electrochemical properties, under continuous dynamic operations of forceful bending (90°) and twisting (180°). More detailed information on electrochemical performance of the as-prepared device under dynamic operations can be seen in Supplementary Movie 3.

performances of the all-solid-state supercapacitors. The specific power and energy densities for our bamboo-like carbon nanofibers are 61.3 kW/kg and 2.37 Wh/kg, respectively. These values are larger or comparable than those typical carbon based active materials for supercapacitors (e.g., 23 kW/kg and 6 Wh/kg for single-walled carbon nanotubes,<sup>33</sup> 4 kW/kg and 0.2 Wh/kg for active carbon cloth<sup>34</sup>). Moreover, compared with many of the previous work, our bamboo-like carbon nanofiber membranes can work as free-standing electrodes for an all-solid-state supercapacitor. Without the need for extra support, the energy and power densities based on the total mass and volume of the devices are improved greatly. A Ragone plot, shown in Figure 5f, compares the volumetric power and energy densities of the as-prepared device with other energy storage

devices designed for high-performance microelectronics, as well as a commercial 2.75/44 mF active carbon electrochemical capacitors (AC-EC), a 500  $\mu$ Ah thin-film lithium battery and a 3 V/300  $\mu$ F aluminum electrolytic capacitor. The highest energy density of the as-made all-solid-state supercapacitor is  $2.4 \times 10^{-4}$  W h cm<sup>-3</sup> with a high power density of 6.1 W cm<sup>-3</sup>. This value is much larger than those typical all-solid-state electrochemical capacitors based on graphene ( $6 \times 10^{-5}$  W h cm<sup>-3</sup>)<sup>1</sup> and single-walled carbon nanotubes (SCNTs,  $1 \times 10^{-5}$  W h cm<sup>-3</sup>).<sup>33</sup> Furthermore, the as-made device exhibits better or comparable energy density with a typical metal oxide-based all-solid-state supercapacitor (e.g., device with H-TiO<sub>2</sub>@MnO<sub>2</sub>/H-TiO<sub>2</sub>@C electrodes),<sup>30</sup> metal nitride-based all-solid-state supercapacitor [e.g., device with mesoporous vanadium

nitride nanowire-carbon nanotube (MVNN-CNTs) electrodes]<sup>35</sup> and conducting polymer-based all-solid-state supercapacitor [e.g., devices with polypyrrole-paper (PPy-paper) electrodes]<sup>36</sup> but much better power density. Compared with the 500  $\mu\text{Ah}$  thin-film lithium battery with low power density and 3 V/300  $\mu\text{F}$  aluminum electrolytic capacitor with low energy density, our device exhibits both high power and energy density, which are also much better than that of the commercial AC-EC. The ability to achieve a high volume/mass capacitance in our work further confirms the importance of the use of self-supporting electrodes without extra current collectors or flexible substrates. This will reduce the device thickness and weight and directly enable us to achieve much larger overall capacitance.

Achieving superior electrochemical performances while maintaining the flexible quality of the supercapacitors is essential to power portable electronic devices and smart garments.<sup>37</sup> The prepared all-solid-state supercapacitor is robust enough to work under different mechanical deformation conditions without degradation in performance. Almost 100% capacitance retention ratio, calculated based on CV curves, was observed for the as-prepared device under continuous dynamic operations of forceful bending and twisting (90°, 180°), and back to the initial status (Figure Sg, Supporting Information, Movie S3), demonstrating the superior mechanical durability and electrochemical stability. SEM results indicate that even after 10 000 charge/discharge cycles, as well as in situ bending and twisting operations, the initial structure of an as-made device is well-maintained, again confirming its outstanding structural stability and mechanical durability (Supporting Information, Figure S13). Specifically, the electrochemical performances of the all-solid-state supercapacitors may be further improved by introducing nanosized pseudocapacitive active materials (e.g.,  $\text{MnO}_2$ ) into the as-formed carbon nanofiber system, which will open the possibility for assembling all-solid-state devices that meet the requirements of commercialization. Our nature-inspired work extends the research frontier on flexible all-solid-state supercapacitors, and opens up new paths to accelerate the development of their advanced applications.

## ■ ASSOCIATED CONTENT

### Supporting Information

Experimental details, additional figures and movies. The Supporting Information is available free of charge on the ACS Publications website at DOI: 10.1021/acs.nanolett.5b00738.

## ■ AUTHOR INFORMATION

### Corresponding Authors

\*E-mail: huxl@mail.hust.edu.cn (X.H.).

\*E-mail: huangyh@mail.hust.edu.cn (Y. H.).

\*E-mail: yicui@stanford.edu (Y. C.).

### Notes

The authors declare no competing financial interest.

## ■ ACKNOWLEDGMENTS

This work is supported by Samsung Electronics. Y.H. acknowledges the support from Program for Changjiang Scholars and Innovative Research Team in University (No. IRT1014). X.H. acknowledges the support from the National Natural Science Foundation of China (No. 21271078 and

51472098). R.S. acknowledges the support of Sandia National Laboratories. Sandia National Laboratories is a multiprogram laboratory managed and operated by Sandia Corporation, a wholly owned subsidiary of Lockheed Martin Corporation, for the U.S. Department of Energy's National Nuclear Security Administration under Contract DE-AC04-94AL85000. Z.Z. acknowledges the support from the National Natural Science Foundation of China (No. 21477046). The authors thank Analytical and Testing Center of HUST for TEM measurements. Mr. David Gilley (Micromeritics Instrument Corporation) is acknowledged for helpful discussion and instruction in nitrogen sorption analysis.

## ■ REFERENCES

- (1) El-Kady, M. F.; Strong, V.; Dubin, S.; Kaner, R. B. Laser scribing of high-performance and flexible graphene-based electrochemical capacitors. *Science* **2012**, *335*, 1326–1330.
- (2) Gao, W.; Singh, N.; Song, L.; Liu, Z.; Reddy, A. L. M.; Ci, L. J.; Vajtai, R.; Zhang, Q.; Wei, B. Q.; Ajayan, P. M. Direct laser writing of micro-supercapacitors on hydrated graphite oxide films. *Nat. Nanotechnol.* **2011**, *6*, 496–500.
- (3) Yu, D. S.; Goh, K. L.; Wang, H.; Wei, L.; Jiang, W. C.; Zhang, Q.; Dai, L. M.; Chen, Y. Scalable synthesis of hierarchically structured carbon nanotube-graphene fibres for capacitive energy storage. *Nat. Nanotechnol.* **2014**, *9*, 555–562.
- (4) Choi, B. G.; Hong, J.; Hong, W. H.; Hammond, P. T.; Park, H. Facilitated ion transport in all-solid-state flexible supercapacitors. *ACS Nano* **2011**, *5*, 7205–7213.
- (5) Lu, X. H.; Zhai, T.; Zhang, X. H.; Shen, Y. Q.; Yuan, L. Y.; Hu, B.; Gong, L.; Chen, J.; Gao, Y. H.; Zhou, J.; Tong, Y. X.; Wang, Z. L.  $\text{WO}_{3-x}$ @Au@ $\text{MnO}_2$  core-shell nanowires on carbon fabric for high-performance flexible supercapacitors. *Adv. Mater.* **2012**, *24*, 938–944.
- (6) Chen, L. F.; Huang, Z. H.; Liang, H. W.; Yao, W. T.; Yu, Z. Y.; Yu, S. H. Flexible all-solid-state high-power supercapacitor fabricated with nitrogen-doped carbon nanofiber electrode material derived from bacterial cellulose. *Energy Environ. Sci.* **2013**, *6*, 3331–3338.
- (7) El-Kady, M. F.; Kaner, R. B. Scalable fabrication of high-power graphene micro-supercapacitors for flexible and on-chip energy storage. *Nat. Commun.* **2013**, *4*, 1475.
- (8) Peng, X.; Peng, L. L.; Wu, C. Z.; Xie, Y. Two dimensional nanomaterials for flexible supercapacitors. *Chem. Soc. Rev.* **2014**, *43*, 3303–3323.
- (9) Beidaghi, M.; Gogotsi, Y. Capacitive energy storage in micro-scale devices: recent advances in design and fabrication of micro-supercapacitors. *Energy Environ. Sci.* **2014**, *7*, 867–884.
- (10) Lu, X. H.; Yu, M. H.; Wang, G. M.; Tong, Y. X.; Li, Y. Flexible solid-state supercapacitors: design, fabrication and applications. *Energy Environ. Sci.* **2014**, *7*, 2160–2181.
- (11) Xie, K. Y.; Wei, B. Q. Materials and structures for stretchable energy storage and conversion devices. *Adv. Mater.* **2014**, *26*, 3592–3617.
- (12) Ahn, J. H.; Je, J. H. Stretchable electronics: materials, architectures and integrations. *J. Phys. D: Appl. Phys.* **2012**, *45*, 103001.
- (13) Xu, Y. X.; Lin, Z. Y.; Huang, X. Q.; Liu, Y.; Huang, Y.; Duan, X. F. Flexible solid-state supercapacitors based on three-dimensional graphene hydrogel films. *ACS Nano* **2013**, *7*, 4042–4049.
- (14) Li, M.; Tang, Z.; Leng, M.; Xue, J. M. Flexible solid-state supercapacitor based on graphene-based hybrid films. *Adv. Funct. Mater.* **2014**, *24*, 7495–7502.
- (15) Sun, H.; You, X.; Deng, J.; Chen, X. L.; Yang, Z. B.; Ren, J.; Peng, H. S. Novel Graphene/Carbon Nanotube Composite Fibers for Efficient Wire-Shaped Miniature Energy Devices. *Adv. Funct. Mater.* **2014**, *26*, 2868–2873.
- (16) Choi, C.; Lee, J. A.; Choi, A. Y.; Kim, Y. T.; Lepró, X.; Lima, M. D.; Baughman, R. H.; Kim, S. J. Flexible supercapacitor made of carbon nanotube yarn with internal pores. *Adv. Mater.* **2013**, *26*, 2059–2065.

(17) Amada, S.; Ichikawa, Y.; Munekata, T.; Nagase, Y.; Shimizu, H. Fiber texture and mechanical graded structure of bamboo. *Compos. Part B: Eng.* **1997**, *28*, 13–20.

(18) Tan, T.; Rahbar, N.; Allameh, S. M.; Kwofie, S.; Dissmore, D.; Ghavami, K.; Soboyejo, W. O. Mechanical properties of functionally graded hierarchical bamboo structures. *Acta Biomater.* **2011**, *7*, 3796–3803.

(19) Silva, E. C. N.; Walters, M. C.; Paulino, G. H. Modeling bamboo as a functionally graded material: lessons for the analysis of affordable materials. *J. Mater. Sci.* **2006**, *41*, 6991–7004.

(20) Gogotsi, Y.; Nikitin, A.; Ye, H. H.; Zhou, W.; Fischer, J. E.; Yi, B.; Foley, H. C.; Barsoum, M. W. Nanoporous carbide-derived carbon with tunable pore size. *Nat. Mater.* **2003**, *2*, 591–594.

(21) Simon, P.; Gogotsi, Y. Materials for electrochemical capacitors. *Nat. Mater.* **2008**, *7*, 845–854.

(22) Zhu, Y. W.; Murali, S.; Stoller, M. D.; Ganesh, K. J.; Cai, W. W.; Ferreira, P. J.; Pirkle, A.; Wallace, R. M.; Cyhosh, K. A.; Thommes, M.; Su, D.; Stach, E. A.; Ruoff, R. S. Carbon-based supercapacitors produced by activation of graphene. *Science* **2011**, *332*, 1537–1541.

(23) Chmiola, J.; Largeot, C.; Taberna, P. L.; Simon, P.; Gogotsi, Y. Monolithic carbide-derived carbon films for micro-supercapacitors. *Science* **2010**, *328*, 480–483.

(24) Yang, X. W.; Cheng, C.; Wang, Y. F.; Qiu, L.; Li, D. Liquid-mediated dense integration of graphene materials for compact capacitive energy storage. *Science* **2013**, *341*, 534–537.

(25) Zimmerman, R. W. Elastic moduli of a solid containing spherical inclusions. *Mech. Mater.* **1991**, *12*, 17–24.

(26) Rice, R. W. *Porosity of Ceramics*; Marcel Dekker: New York, 1998.

(27) Frackowiak, E.; Béguin, F. Carbon materials for the electrochemical storage of energy in capacitors. *Carbon* **2001**, *39*, 937–950.

(28) Lee, S. W.; Gallant, B. M.; Byon, H. R.; Hammond, P. T.; Shao-Horn, Y. Nanostructured carbon-based electrodes: bridging the gap between thin-film lithium-ion batteries and electrochemical capacitors. *Energy Environ. Sci.* **2011**, *4*, 1972–1985.

(29) Pech, D.; Brunet, M.; Durou, H.; Huang, P. H.; Mochalin, V.; Gogotsi, Y.; Taberna, P. L.; Simon, P. Ultrahigh-power micrometre-sized supercapacitors based on onion-like carbon. *Nat. Nanotechnol.* **2010**, *5*, 651–654.

(30) Lu, X. H.; Yu, M. H.; Wang, G. M.; Zhai, T.; Xie, S. L.; Ling, Y. C.; Tong, Y. X.; Li, Y. H-TiO<sub>2</sub>@MnO<sub>2</sub>/H-TiO<sub>2</sub>@C core-shell nanowires for high performance and flexible asymmetric supercapacitors. *Adv. Mater.* **2013**, *25*, 267–272.

(31) Xiao, X.; Li, T. Q.; Yang, P. H.; Gao, Y.; Jin, H. Y.; Ni, W. J.; Zhan, W. H.; Zhang, X. H.; Cao, Y. Z.; Zhong, J. W.; Gong, L.; Yen, W. C.; Mai, W. J.; Chen, J.; Huo, K. F.; Chueh, Y. L.; Wang, Z. L.; Zhou, J. Fiber-based all-solid-state flexible supercapacitors for self-powered systems. *ACS Nano* **2012**, *6*, 9200–9206.

(32) Wang, D. W.; Li, F.; Liu, M.; Lu, G. Q.; Cheng, H. M. 3D aperiodic hierarchical porous graphitic carbon material for high-rate electrochemical capacitive energy storage. *Angew. Chem., Int. Ed.* **2008**, *47*, 373–376.

(33) Kaempgen, M.; Chan, C. K.; Ma, J.; Cui, Y.; Gruner, G. Printable thin film supercapacitors using single-walled carbon nanotubes. *Nano Lett.* **2009**, *9*, 1872–1876.

(34) Yan, J.; Wang, Q.; Wei, T.; Jiang, L. L.; Zhang, M. L.; Jing, X. Y.; Fan, Z. J. Template-assisted low temperature synthesis of functionalized graphene for ultrahigh volumetric performance supercapacitors. *ACS Nano* **2014**, *8*, 4720–4729.

(35) Xiao, X.; Peng, X.; Jin, H. Y.; Li, T. Q.; Zhang, C. C.; Gao, B.; Hu, B.; Huo, K. F.; Zhou, J. Supercapacitors: freestanding mesoporous VN/CNT hybrid electrodes for flexible all-solid-state supercapacitors. *Adv. Mater.* **2013**, *25*, 4954–4954.

(36) Yuan, L. Y.; Yao, B.; Hu, B.; Huo, K. F.; Chen, W.; Zhou, J. Polypyrrole-Coated Paper for Flexible Solid-State Energy Storage. *Energy Environ. Sci.* **2013**, *6*, 470–476.

(37) Jost, K.; Perez, C. R.; McDonough, J. K.; Presser, V.; Heon, M.; Dion, G.; Gogotsi, Y. Carbon coated textiles for flexible energy storage. *Energy Environ. Sci.* **2011**, *4*, 5060–5067.